UCSF
UC San Francisco Previously Published Works

Title

HIV-2 Depletes CD4 T Cells through Pyroptosis despite Vpx-Dependent Degradation of SAMHD1

Permalink

https://escholarship.org/uc/item/9t1389g1

Journal

Journal of Virology, 93(24)

ISSN

0022-538X

Authors

Luo, Xiaoyu
Herzig, Eytan
Doitsh, Gilad
et al.

Publication Date

2019-12-01

DOI

10.1128/jvi.00666-19

Peer reviewed

eScholarship.org Powered by the California Digital Library
University of California

AMERICAN SOCIETY FOR MICROBIOLOGY | Journal of Virology®

VIRUS-CELL INTERACTIONS

HIV-2 Depletes CD4 T Cells through Pyroptosis despite Vpx-Dependent Degradation of SAMHD1

Xiaoyu Luo,[a] Eytan Herzig,[a] Gilad Doitsh,[a] Zachary W. Grimmett,[a] Isa Muñoz-Arias,[a] Warner C. Greene[a,b,c]

[a]Gladstone Institute of Virology and Immunology, University of California, San Francisco, San Francisco, California, USA
[b]Department of Medicine, University of California, San Francisco, San Francisco, California, USA
[c]Department of Microbiology and Immunology, University of California, San Francisco, San Francisco, California, USA

ABSTRACT Human immunodeficiency virus type 2 (HIV-2) infection results in a milder course of disease and slower progression to AIDS than does HIV-1. We hypothesized that this difference may be due to degradation of the sterile alpha motif and HD domain 1 (SAMHD1) host restriction factor by the HIV-2 Vpx gene product, thereby diminishing abortive infection and pyroptotic cell death within bystander CD4 T cells. We have compared CD4 T cell death in tonsil-derived human lymphoid aggregate cultures (HLACs) infected with wild-type HIV-2, HIV-2 ΔVpx, or HIV-1. In contrast to our hypothesis, HIV-2, HIV-2 ΔVpx, and HIV-1 induced similar levels of bystander CD4 T cell death. In all cases, cell death was blocked by AMD3100, a CXCR4 entry inhibitor, but not by raltegravir, an integrase, indicating that only early life cycle events were required. Cell death was also blocked by a caspase-1 inhibitor, a key enzyme promoting pyroptosis, but not by a caspase-3 inhibitor, an important enzyme in apoptosis. HIV-1-induced abortive infection and pyroptotic cell death were also not reduced by forced encapsidation of HIV-2 Vpx into HIV-1 virions. Together, these findings indicate that HIV-2 and HIV-1 support similar levels of CD4 T cell depletion *in vitro* despite HIV-2 Vpx-mediated degradation of the SAMHD1 transcription factor. The milder disease course observed with HIV-2 infection likely stems from factors other than abortive infection and caspase-1-dependent pyroptosis in bystander CD4 T cells.

IMPORTANCE CD4 T cell depletion during HIV-1 infection involves the demise of bystander CD4 T cells due to abortive infection, viral DNA sensing, inflammasome assembly, and death by caspase-1-dependent pyroptosis. HIV-2 infection is associated with milder disease and lower rates of CD4 T cell loss. We hypothesized that HIV-2 infection produces lower levels of pyroptosis due to the action of its Vpx gene product. Vpx degrades the SAMHD1 restriction factor, potentially reducing abortive forms of infection. However, in tonsil cell cultures, HIV-2, HIV-2 ΔVpx, and HIV-1 induced indistinguishable levels of pyroptosis. Forced encapsidation of Vpx into HIV-1 virions also did not reduce pyroptosis. Thus, SAMHD1 does not appear to play a key role in the induction of bystander cell pyroptosis. Additionally, the milder clinical course of HIV-2-induced disease is apparently not explained by a decrease in this inflammatory form of programmed cell death.

KEYWORDS AIDS, HIV-1, HIV-2, pyroptosis, SAMHD1, cell death

The progressive loss of CD4 T cells during untreated HIV-1 infection underlies clinical progression to AIDS (1–4). However, HIV-1 is not the only type of human immunodeficiency virus infecting CD4 T cells. HIV-2 is primarily found within West Africa (Guinea-Bissau, The Gambia, Senegal, Cape Verde, Côte d'Ivoire, Mali, Sierra Leone, and Nigeria) with some spread due to globalization. Compared to HIV-1, HIV-2 generally causes a less virulent form of infection, with substantially lower levels of viremia (5–10),

Citation Luo X, Herzig E, Doitsh G, Grimmett ZW, Muñoz-Arias I, Greene WC. 2019. HIV-2 depletes CD4 T cells through pyroptosis despite Vpx-dependent degradation of SAMHD1. J Virol 93:e00666-19. https://doi.org/10.1128/JVI.00666-19.

Editor Frank Kirchhoff, Ulm University Medical Center

Copyright © 2019 American Society for Microbiology. All Rights Reserved.

Address correspondence to Warner C. Greene, warner.greene@gladstone.ucsf.edu.

Received 25 April 2019
Accepted 11 September 2019
Accepted manuscript posted online 2 October 2019
Published 26 November 2019

a slower decline in CD4 T cell counts, and a better long-term prognosis. A 1997 study with a median follow-up time of 2.1 years concluded that the overall annual rate of CD4 T cell decline is −2.1% in HIV-1 patients and −1.08% in HIV-2 patients (11). In addition, the majority of HIV-2-infected individuals never progress to frank AIDS (12, 13). However, in cases where immunodeficiency does develop in HIV-2-infected individuals, high mortality rates occur in the absence of treatment (10, 14). Dual infection with HIV-1 and HIV-2 can occur and is thought to delay the progression of HIV-1 disease; however, prior infection with HIV-2 does not appear to protect against HIV-1 infection (15, 16).

What underlies the more benign clinical course of HIV-2 infection compared to HIV-1? One possibility relates to the fact that HIV-2 encodes an additional gene, Vpx, that is not present in HIV-1. Vpx targets a major host restriction factor, sterile alpha motif and HD domain 1 (SAMHD1), for proteasomal degradation (17–21). SAMHD1 restricts the growth of HIV in resting CD4 T cells (18, 22, 23). SAMHD1 acts by lowering the cytoplasmic pool of deoxynucleoside triphosphates (dNTPs), thus compromising HIV-1 reverse transcription (24–26). Vpx targets SAMHD1 for ubiquitylation and proteasomal degradation (17), resulting in increased dNTP levels and enhanced reverse transcription (20, 22). It is also intriguing that many primate viruses encoding Vpx exhibit low pathogenicity in their natural hosts (21, 27, 28). Together, these findings raise the possibility that Vpx might play a key role in the diminished pathogenicity of HIV-2 in humans.

In addition to SAMHD1, Vpx also promotes the degradation of the human silencing hub (HUSH) complex that recruits the H3K9me3 methyltransferase SET domain bifurcated 1 (SETDB1)-mediated epigenetic silencing (29). However, the restrictive effects of this complex are likely exerted after proviral integration.

Recent studies performed with cells from human tonsil indicate that approximately 5% of the resident CD4 T cells are sufficiently activated to undergo productive infection with HIV-1. After producing new virions, these cells die by caspase-3-dependent apoptosis, a noninflammatory form of programmed cell death. Conversely, the remaining 95% of CD4 T cells present in tonsils are quiescent and thus refractory to productive HIV-1 infection (30–32). Following cell-to-cell transmission of virus to these nonpermissive cells (33), abortive infection occurs, leading to the accumulation of incomplete viral reverse transcription products. These "foreign" DNAs are sensed by the host IFI16 protein (34), which in turn promotes inflammasome assembly, and caspase-1 activation leading to pyroptosis, a highly inflammatory form of programmed cell death (34). The molecular underpinnings of diminished reverse transcription in these nonpermissive bystander cells are unclear but could be linked to SAMHD1-mediated reduction in deoxynucleotide triphosphate levels.

We hypothesized that SAMHD1-mediated inhibition of reverse transcription plays a major role in the accumulation of incomplete viral transcripts in abortively infected CD4 T cells in lymphoid tissue. Vpx antagonism of SAMHD1 function during HIV-2 infection could reduce levels of abortive infection, DNA sensing, inflammasome assembly, and pyroptosis (23, 35). Many prior studies investigating the biological effects of SAMHD1 employed CD4 T cells derived from blood; however, because these blood cells are naturally resistant to pyroptosis (36), our studies have focused on lymphoid tissue-derived tonsil cells to test whether HIV-2 Vpx-mediated degradation of SAMHD1 reduces abortive infection and pyroptotic death of CD4 T cells. Such an effect could potentially account for the milder clinical disease course produced by this virus.

RESULTS

Tonsil CD4 T cells express high levels of functional SAMHD1. Bystander CD4 T cell depletion in the presence of HIV-1 was studied using an *ex vivo* human lymphoid aggregate culture (HLAC) system prepared using fresh human tonsil specimens (30, 31). As noted, HIV-2, but not HIV-1, encodes Vpx that can target the SAMHD1 restriction factor for polyubiquitylation and proteasome-mediated degradation. Loss of SAMHD1 might relieve abortive HIV-1 infection that triggers pyroptotic CD4 T cell death. To study this possibility, SAMHD1 expression and key changes in its phosphorylation state

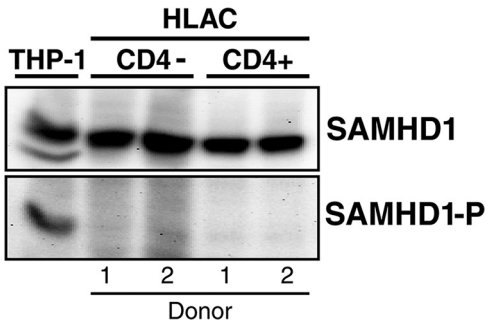

FIG 1 SAMHD1 viral restriction factor is highly expressed in an unphosphorylated form in tonsil CD4$^+$ and CD4$^-$ T cells. *Ex vivo* human lymphoid aggregate cultures (HLACs) were prepared using tonsil tissue from two different donors. CD4$^+$ and CD4$^-$ T cells were isolated and whole-cell lysates prepared, followed by SDS-polyacrylamide gel electrophoresis (SDS-PAGE) and immunoblotting with anti-SAMHD1 antibodies (top row) or anti-phospho-Thr592-SAMHD1 (bottom row). Phosphorylation at this site inactivates SAMHD1 (37). THP-1 cells were incorporated as a positive control for reactivity of the anti-phospho-SAMHD1 antibody. Similar results were obtained with three additional donors.

were studied in CD4$^+$ and CD4$^-$ tonsil T cells purified from two different donors (Fig. 1). THP-1 monocytic cells were included as a positive control. Comparable levels of SAMHD1 were readily detected in the two donors in both the CD4$^+$ and CD4$^-$ cells (Fig. 1, top). The anti-HIV activity of SAMHD1 is downregulated following cyclin A2/CDK1-mediated phosphorylation on Thr-592, which can be detected by immunoblotting with a specific anti-phospho-Thr-592 SAMHD1 antibody (24, 37). Neither the CD4$^+$ nor CD4$^-$ tonsil cells contained detectable levels of phosphorylated SAMHD1, while THP-1 cells did contain phosphorylated SAMHD1 (Fig. 1, bottom). Together, these findings indicate that both CD4$^+$ and CD4$^-$ tonsil cells express high levels of SAMHD1, and based on the lack of phosphorylation at Thr-592, these SAMHD1 proteins are predicted to function as viral restriction factors.

Vpx-dependent degradation of SAMHD1 enhances permissivity to HIV infection and depletion of CD4 T cells. To test whether Vpx degrades SAMHD1 in HLAC CD4 T cells, these cells were spinoculated with HIV-1 (NLENG1-IRES), HIV-2 (ROD2-GFP; GFP, green fluorescent protein), or HIV-2 ΔVpx (ROD2-ΔVPX-GFP) at the same multiplicity of infection (MOI). Cells were cultured for 2 to 6 days until productive infection, and bystander cell loss was observed (Fig. 2A). SAMHD1 and phosphorylated forms of this restriction factor were then assessed by immunoblotting (Fig. 2B and C). Unstimulated THP-1 cells expressing phospho-SAMHD1 or phorbol myristate acetate (PMA)-stimulated THP-1 cells, which lose phospho-SAMHD1 following phorbol ester-induced cell differentiation, were included as controls. Surprisingly, although the level of productive infection was less than 10% in the tonsil CD4 T cells, SAMHD1 levels were undetectable after HIV-2 infection. SAMHD1 was readily detected in cells infected with HIV-2 ΔVpx or HIV-1 (Fig. 2B). Based on Image J quantitation of SAMHD1 and β-actin, the modest decrease in SAMHD1 in HIV-2 ΔVpx-infected cells was due to slightly lower overall protein loading (data not shown). While PMA stimulation of THP-1 cells impaired phosphorylation of SAMHD1, no evidence of SAMHD1 phosphorylation was detected in any of the infected HLAC samples (Fig. 2C). Together, these findings indicate that HIV-2 Vpx is biologically active and capable of degrading SAMHD1 in both productively infected and abortively infected bystander tonsil CD4 T cells. In contrast, neither HIV-2 ΔVpx nor HIV-1 depletes SAMHD1, and this restriction factor is not inactivated by phosphorylation on Thr-592 in the tonsil cells.

Next, we assessed the impact of HIV-2 Vpx-mediated degradation of SAMHD1 on productive viral replication and bystander CD4 T cell depletion. HLACs were spinoculated with HIV-1, HIV-2, or HIV-2 ΔVpx at the same MOI and cultured for 2 to 6 days. Cells were analyzed by flow cytometry to determine levels of CD4, CD8, and CD2 (a surrogate T cell marker employed because HIV-2 Nef can downregulate CD3 (38) (see Fig. S2 in the supplemental material). Productively infected cells were identified by GFP

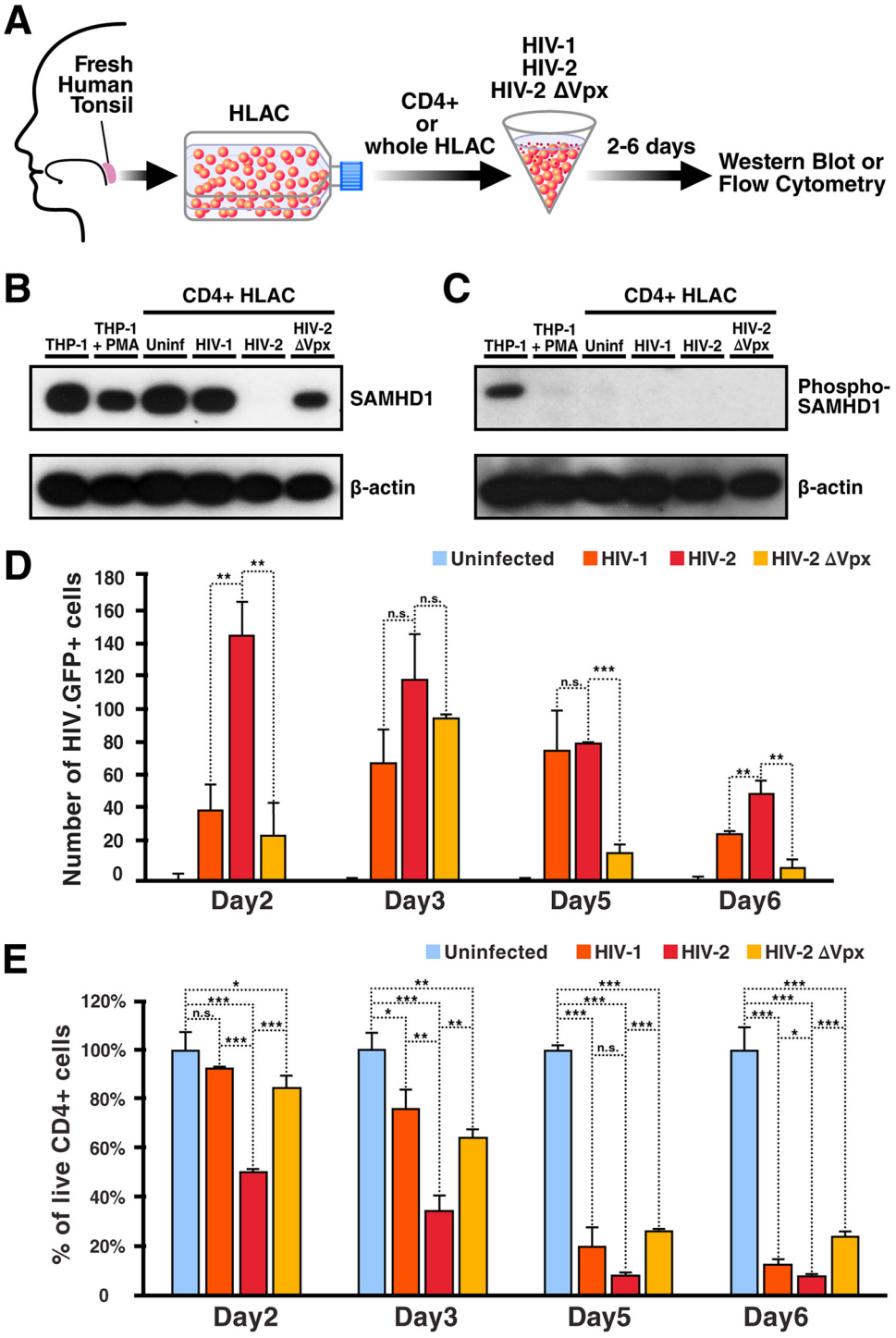

FIG 2 Vpx-dependent degradation of SAMHD1 enhances productive HIV-2 infection and depletion of bystander tonsil CD4 T cells. (A) Schematic summary of spinoculation protocol for infection of tonsil cells. Tonsil HLACs or $CD4^+$ cells isolated from HLACs were spinoculated with replication-competent HIV-1, HIV-2, or HIV-2 ΔVpx, each encoding a GFP reporter. Viral inputs were normalized based on the $TCID_{50}$ determined in TZM-bl assays. HLAC or $CD4^+$ cells were collected at days 2, 3, 5, and 6 after infection and analyzed by flow cytometry and immunoblotting. (B and C) For the immunoblotting studies, cell extracts from the virally infected HLAC $CD4^+$ cells were immunoblotted with anti-SAMHD1 and anti-β-actin (protein loading control) (B) or anti-phospho-Thr592-SAMHD1 and anti-β-actin (C) antibodies. Uninf, uninfected. This experiment was repeated three times with tonsil tissue from different donors, with similar results. (D) Time course of the appearance of productively infected (GFP^+) cells following HIV-1, HIV-2, and HIV-2 ΔVpx infection by spinoculation on day 0. Values represent mean + standard deviation (SD), as determined in triplicate samples measured by flow cytometry. Note the significantly higher number of productively infected cells following HIV-2 infection. (E) Time course of the percentage of live CD4 T cells

(Continued on next page)

epifluorescence. Up to a ~4-fold increase in productive infection was observed in HIV-2-infected HLACs compared to HIV-1- or HIV-2 ΔVpx-infected HLACs at day 2 (Fig. 2D and S2E). Compared to HIV-2 ΔVpx, HIV-2 infection resulted in a significantly greater number and percentage of productively infected HLAC cells on days 2, 5, and 6 of the time course (Fig. 2D and S2E). Productive infection with HIV-1 also occurred more slowly than with HIV-2. Together, these findings suggest that the action of the Vpx protein enhanced permissivity of the resting tonsillar CD4 T cells to early productive infection.

However, counter to our initial hypothesis that the degradation of SAMHD1 by Vpx in bystander cells would result in a less-pathogenic form of infection, we detected more T cell depletion in HIV-2-infected HLACs than in HIV-2 ΔVpx- or HIV-1-infected cultures (Fig. 2E and S2A to D). However, the fact that the presence of Vpx was associated with higher levels of productive infection complicates the interpretation of these results. Higher levels of early productive infection (see day 2, Fig. 2D) could result in higher levels of abortive infection in bystander cells and increased cell death (see day 3, Fig. 2E) than in cultures infected with HIV-2 ΔVpx. Ultimately, bystander cells are markedly depleted in all of the cultures (see day 6, Fig. 2E). Overall, these results suggest that the Vpx-induced degradation of SAMHD1 does not attenuate HIV-2-mediated T cell depletion, but the increased number of productively infected cells present early in the HIV-2-infected cultures complicates an interpretation of the results.

Vpx-induced degradation of SAMHD1 also does not decrease HIV-2-dependent T cell depletion in a 293T HLAC overlay system. In order to assess killing following HIV-2, HIV-2 ΔVpx, and HIV-1 infection in a system where the numbers of productively infected cells are equivalent, we turned to the 293T HLAC overlay system, as previously described (Fig. 3) (33). Our prior findings with HIV-1 indicated that pyroptotic death of bystander CD4 T cells required cell-to-cell transmission of HIV-1 from productively infected cells to the bystander cells (33). Infection with cell-free virions, which is 100- to 1,000-fold less efficient (39, 40), was not sufficient to induce bystander cell death. The 293T overlay system allows the production of an equivalent number of HIV-producing 293T cells for cell-to-cell transmission to the overlying tonsil CD4 T cells. To further confirm comparable production of infectious virus by the transfected 293T cells, supernatants from these cultures were tested in TZM-bl assays. These studies confirmed the presence of statistically indistinguishable titers of HIV-2, HIV-2 ΔVpx, and HIV-1 (data not shown).

In studies involving the overlay of tonsil-derived lymphocytes, we routinely included raltegravir, an integrase inhibitor, to ensure that virus transmission from the 293T to HLAC cells did not lead to a productive and spreading infection within the overlaid tonsil CD4 T cells. Using this system, we first confirmed by intracellular immunostaining and flow cytometry that HIV-2, but not HIV-2 ΔVpx or HIV-1, downregulated the expression of SAMHD1 in CD4 T cells (Fig. 3B and D). As expected, SAMHD1 levels did not change in $CD2^+$ $CD8^+$ T cells infected with HIV-2 or HIV-2 ΔVpx or HIV-1, consistent with the insusceptibility of these cells to infection by these viruses. The flow cytometric results were further confirmed by immunoblotting extracts from these cultures with anti-SAMHD1 antibodies (Fig. 3C).

When bystander CD4 T cell depletion was assessed in these cultures, the HIV-1-, HIV-2-, and HIV-2ΔVpx-infected cultures exhibited statistically indistinguishable levels of bystander CD4 T cell depletion (Fig. 3E). These findings clearly demonstrate that HIV-2 Vpx-mediated degradation on SAMHD1 does not result in reduced death of bystander CD4 T cells as originally hypothesized.

FIG 2 Legend (Continued)
present on days 2, 3, 5, and 6 after viral infection by spinoculation (day 0). Live cells were defined by sequential gating beginning with Zombie staining to select live lymphocytes, followed by normalization by the number of CD8 T cells recovered. The number of live CD4 T cells present in the uninfected tonsil culture was set as 100% (see Fig. S1 for more details). The time course experiment presented in panels D and E was repeated three times, with similar results. *, $P \leq 0.05$; **, $P \leq 0.005$; ***, $P \leq 0.001$; n.s., not significant.

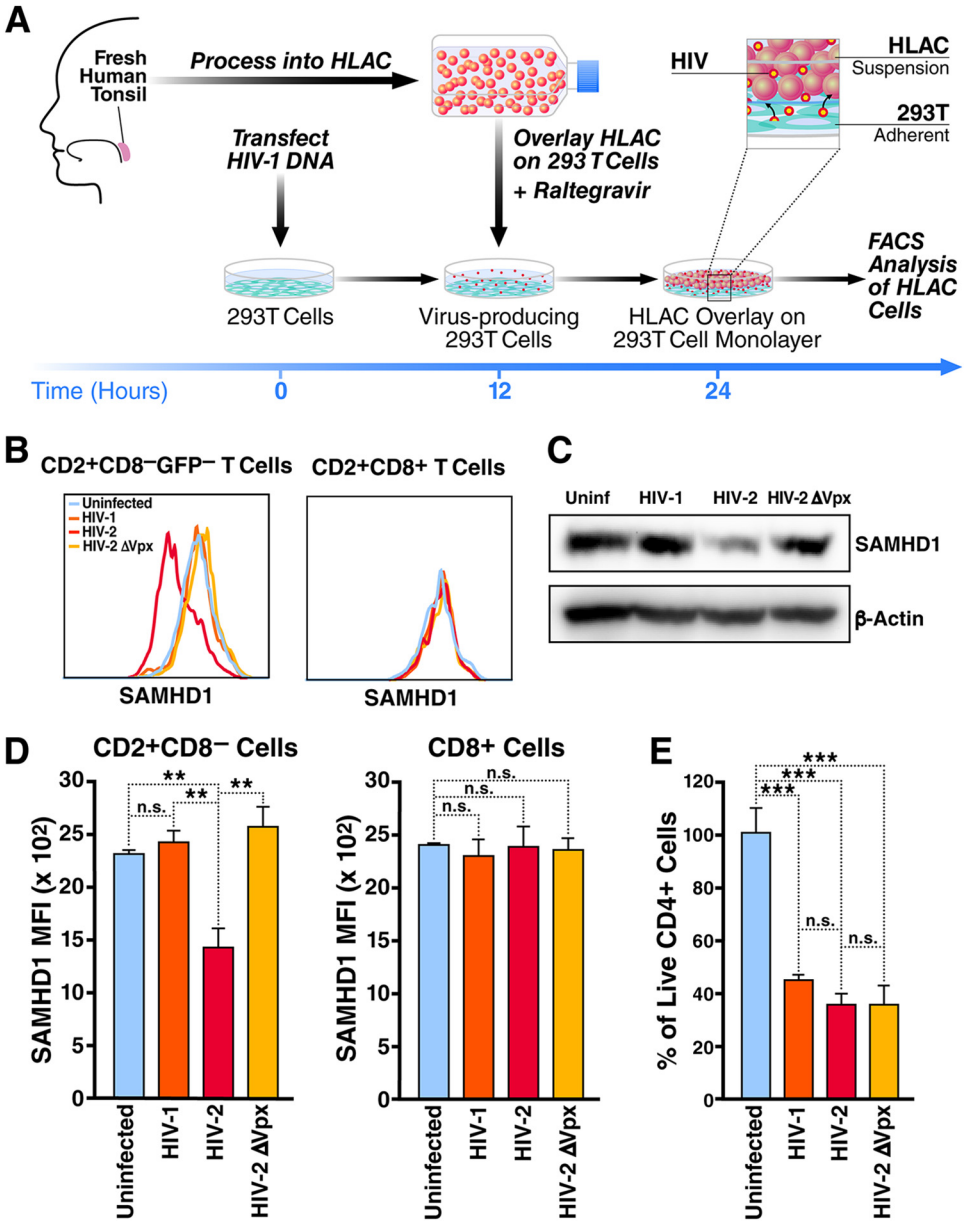

FIG 3 HIV-2 Vpx depletion of SAMHD1 does not reduce depletion of bystander CD4 T cells. (A) Schematic summary of the 293T-tonsil overlay system. As illustrated, fresh human tonsil was processed into HLACs, and cells were cultured in suspension. Simultaneously, 293T cells were transfected with 50 to 100 ng HIV-1 DNA in a 24-well plate. After 12 h, 293T cells were washed and overlaid with 3×10^6 HLAC cells in the presence of raltegravir (15 μM) to prevent spreading infection. Virus-producing 293T cells directly interacted with the overlaid HLAC target cells. After 24 to 48 h, the HLAC suspensions were collected from wells and analyzed by flow cytometry. 293T cells transfected with equivalent amounts of proviral DNA (HIV-1, HIV-2, and HIV-2 ΔVpx) produced comparable amounts of infectious virus, as determined by TZM-bl infectivity assays (data not shown). (B) 293T cells were transfected with 50 ng of HIV-1, HIV-2, or HIV-2 ΔVpx proviral DNA, and a 293T overlay experiment was performed as described in panel A. HLACs were collected at 24 to 48 h postoverlay and stained with a viability dye (Zombie Aqua) and antibodies against CD2, CD4, CD8, and SAMHD1. The histogram depicts the mean fluorescence intensity (MFI) staining for SAMHD1 found in CD4 T cells or CD8 T cells after no infection or infection with HIV-1, HIV-2, or HIV-2 ΔVpx. (C) Anti-SAMHD1 and anti-β-actin immunoblotting was performed 48 h after on purified tonsil $CD4^+$ T cells that had been infected with HIV-1, HIV-2, or HIV-2 ΔVpx in the 293T overlay system. β-Actin was included as a loading control. (D) Quantitation of SAMHD1 staining in $CD2^+$ $CD8^-$ cells and $CD2^+$ $CD8^+$ cells using the mean fluorescence intensity (MFI) + SD from triplicate samples. **, $P \leq 0.005$; ***, $P \leq 0.001$; n.s., not significant. (E) Percentages of viable CD4 T cells 48 h after HLAC overlay on virus-producing 293T cells. Note similar levels of bystander CD4 T cell depletion despite HIV-2 Vpx-mediated degradation of the SAMHD1 restriction factor. Data are representative of 2 independent experiments performed with tonsil tissue from 6 different donors.

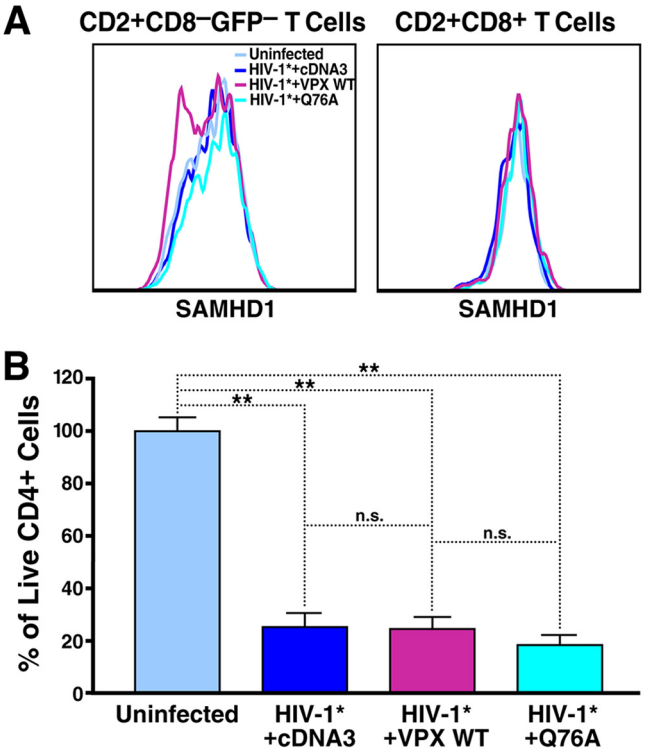

FIG 4 SAMHD1 degradation by exogenous Vpx incorporated into HIV-1 virions does not rescue bystander CD4 T cells from cell death. 293T cells were cotransfected with a Vpx expression vector (pVpx) DNA and DNA from HIV-1*.GFP) that contains a Vpx interaction motif introduced within the Gag p6 protein that promotes encapsidation of Vpx (18) (see Materials and Methods). A 293T-HLAC overlay experiment was performed as described in Fig. 3A. (A) SAMHD1 expression was detected by intracellular immunostaining of bystander CD4 T cells ($CD2^+$ $CD8^-$ GFP^-) and CD8 T cells ($CD2^+$ $CD8^+$) infected with HIV, HIV*Vpx, or HIV*VpxQ76A (a mutation that interferes with Vpx-mediated degradation of SAMHD1) (18, 22, 42). Note the downregulation of SAMHD1 by HIV-1*Vpx but not by HIV-1* or HIV-1*VpxQ76A. (B) The percentage of live $CD4^+$ T cells in each of these cultures was determined. Note that forced encapsidation of Vpx did not alter HIV-1 associated death occurring in bystander cells in these HLACs. Representative data are shown from 4 independent experiments. **, $P \leq 0.005$; n.s., not significant.

Forced encapsidation of Vpx into HIV-1 virions also does not decrease HIV-1-mediated depletion of CD4 T cells. HIV-1 and HIV-2 are divergent viruses that differ in many ways beyond the presence of Vpx in HIV-2 (41). To ensure that our results were not due to other differences in these two viruses, we tested whether direct introduction of simian immunodeficiency virus (SIV) Vpx protein into HIV-1 virions would decrease HIV-1 depletion of bystander CD4 T cells by pyroptosis. To package exogenous Vpx into HIV-1 virions, we used HIV*, which corresponds to a modified version of $HIV\text{-}1_{NL4\text{-}3}$ with a Vpx interaction motif inserted into the Gag p6 region (18). HIV-1 virions containing Vpx wild type (WT) or the Vpx Q76A mutant that does not degrade SAMHD1 due to a lack of binding to the E3 ligase subunit, DCAF1 (18, 22, 42), were produced by cotransfection of both HIV-1* proviral DNA and a Vpx expression vector into 293T cells. In HIV-1*-Vpx-infected but not HIV-1*-VpxQ76A-infected cultures, SAMHD1 expression was decreased in CD4 T cells ($CD2^+$ $CD8^-$) but not in CD8 T cells ($CD2^+$ $CD8^+$) (Fig. 4A). Next, these viruses were used to infect 293T cells overlaid with tonsil cells. Similar levels of bystander CD4 T cell depletion were observed in cultures infected with each of these three viruses. Thus, despite forced encapsidation of Vpx into HIV-1 and effective degradation of SAMHD1, pyroptotic depletion of bystander tonsil CD4 T cells is not altered.

HIV-2 depletion of CD4 T cells appears to involve abortive infection based on effective blocking of cell death by a CXCR4-selective entry inhibitor (AMD3100) but not by an HIV-1/2 integrase inhibitor (raltegravir). Our prior studies demonstrated that the death of nonpermissive bystander CD4 T cells in tonsil HLACs involves

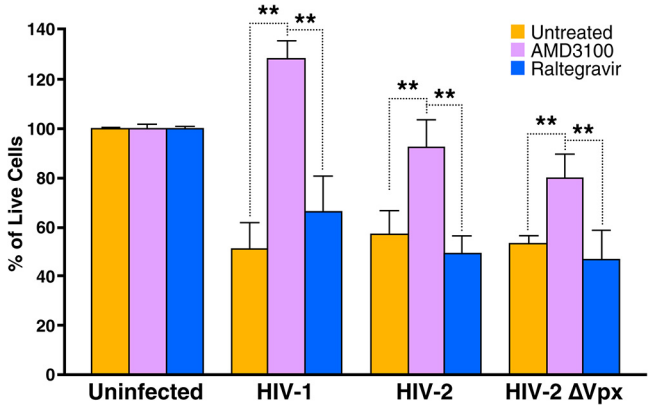

FIG 5 CD4 T cell depletion in both HIV-1- and HIV-2-infected cultures is blocked by AMD3100, a CXCR4 entry inhibitor, but not by raltegravir, an integrase inhibitor. HLACs were treated with AMD3100 (200 μM) or raltegravir (15 μM) before and during overlay with HIV-1-, HIV-2-, or HIV-2 ΔVpx-transfected 293T cells. After 24 to 48 h of culture, HLACs were collected and stained with a viability dye (Zombie Aqua) and antibodies against CD2, CD4, CD8, and SAMHD1. Percentages of live CD4 T cells were defined by calculating the number of CD4 T cells divided by the number of CD8 T cells, or by normalization based on the number of fluorescent beads acquired by volume. The data represent the mean + SD of the results from triplicate samples. **, $P \leq 0.005$. This experiment was repeated three times using tonsil tissue from 9 different donors, with similar results.

abortive viral infection leading to the generation of incomplete reverse transcripts that are detected by the DNA sensor IFI16. A predicted signature of abortive infection as a driver of cell death is the ability of HIV entry inhibitors like AMD3100 to block cell death, while integrase inhibitors like raltegravir do not because their site of action occurs too late to alter DNA sensing of the incomplete reverse transcripts. When HIV-2-associated CD4 T cell depletion was studied in the 293T overlay system, we observed that, as with HIV-1, AMD3100 effectively blocked cell death, while raltegravir did not (Fig. 5). Similar results were obtained when HIV-2 ΔVpx viruses were tested (Fig. 5). Together, these findings are consistent with HIV-2-associated cell death involving early steps in the HIV-2 life cycle, presumably leading to abortive infection of the bystander CD4 T cells as with HIV-1.

HIV-2-associated death of tonsil CD4 T cells is partially reversed by inhibitors of caspase-1 but not caspase-3. Our prior results demonstrated that HIV-1 promotes the death of CD4 T cells present in HLAC cells primarily through caspase-1-dependent pyroptosis. To test if HIV-2-mediated CD4 T cell death is also dependent on caspase-1, HLACs were treated with a caspase-1-selective inhibitor (Z-YVAD-FMK), a caspase-3-selective inhibitor (Z-DEVD-FMK), a pan-caspase inhibitor (Z-VAD-FMK), or dimethyl sulfoxide (DMSO) in 293T overlay experiments. HIV-2-induced death of infected CD4 T cells was significantly rescued by the addition of a caspase-1 inhibitor and a pan-caspase inhibitor but not by the addition of a caspase-3 inhibitor or DMSO (Fig. 6). There was no change in killing levels or rescue patterns between HIV-2 and HIV-2 ΔVPX. These findings are consistent with the conclusion that abortive infection of tonsil CD4 T cells by HIV-2, like HIV-1, induces the death of CD4 T cells by caspase-1-dependent pyroptosis.

DISCUSSION

We have previously shown that a major fraction of the *ex vivo* cell death occurring in HIV-1-infected lymphoid tissues involves "abortive infection" of nonpermissive bystander CD4 T cells (30). Of note, to induce cell death, this infection must occur through cell-to-cell transmission (33), raising the possibility that the infective process must be of sufficient intensity to overcome a natural restriction block present in these nonpermissive bystander cells. Abortive infection gives rise to the accumulation of incomplete reverse transcripts that in turn are detected by the IFI16 DNA sensor (34). IFI16 is the only mammalian sensor known to detect both single- and double-stranded DNA (43).

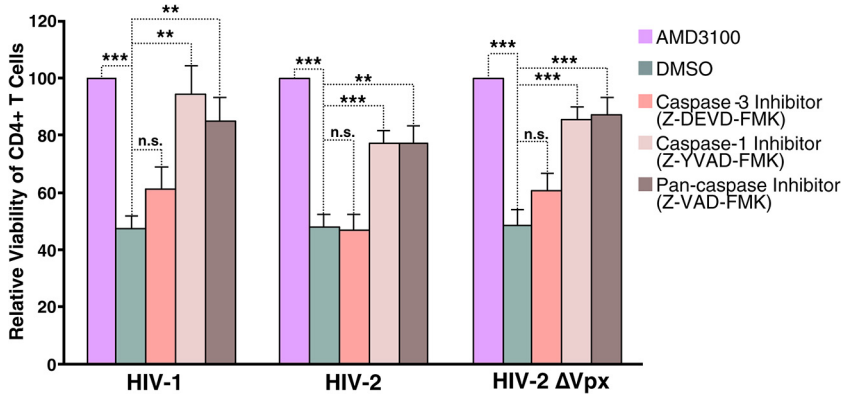

FIG 6 Both HIV-1- and HIV-2-induced CD4 T cell depletion is rescued by AMD3100, caspase-1, and pan-caspase inhibitors but not by caspase-3 inhibition. HLACs were treated with caspase-1 inhibitor (Z-YVAD-FMK, 100 μM), caspase-3 inhibitor (Z-DEVD-FMK, 100 μM), pan-caspase inhibitor (Z-VAD-FMK, 100 μM), and AMD3100 (2 mM) before and during overlay on HIV-1-, HIV-2-, or HIV-2 ΔVpx-transfected 293T cells. HLACs were collected and stained with a viability dye (Zombie violet) and antibodies against CD3, CD4, and CD8. DMSO was used as a solvent control. The relative viability of CD4 T cells was normalized to the number of $CD8^+$ T cells and rescue by AMD. The data represent mean + SD of the results from $n \geq 6$ donors. **, $P \leq 0.005$; ***, $P \leq 0.001$; n.s., not significant. These data are representative of 3 independent experiments.

IFI16 sensing of these viral DNAs leads to inflammasome assembly, activation of caspase-1, and death by pyroptosis, a highly inflammatory form of programmed cell death (31, 32).

SAMHD1 is a major restriction factor for HIV-1 in resting CD4 T cells that acts by lowering intracellular dNTP levels, thereby limiting reverse transcription. HIV-2, but not HIV-1, encodes a Vpx gene product that targets SAMHD1 for ubiquitylation and proteasome-mediated degradation, resulting in increased dNTP levels and enhanced reverse transcription. We were intrigued by the notion that the milder disease course observed in HIV-2-infected individuals could stem from Vpx-mediated degradation of SAMHD1. In this scenario, incomplete viral DNAs would not accumulate for sensing by IFI16. In turn, caspase-1 activation in inflammasomes and pyroptotic cell death would be decreased.

We tested this hypothesis by comparing HIV-1, HIV-2, and HIV-2 ΔVpx infections in the human tonsil tissue-based HLAC system. Vpx expression during HIV-2 infection enhanced productive infection up to ~4-fold compared to that in infections with either HIV-1 or HIV-2 ΔVpx. A similar increase in permissivity has been observed in resting blood CD4 T cells using Vpx containing virus-like particles (VLP-Vpx) that are able to degrade SAMHD1 (35). However, the efficiency of VLP-Vpx is weak compared to HIV-2-induced SAMHD1 degradation in HLAC CD4 T cells (Fig. 2B) (35). This could be the result of our use of a spinoculation method that employs high viral concentrations and an extended centrifugation step to mechanically force viral particles carrying the Vpx protein onto the cells. However, even with undetectable SAMHD1, the shift from abortive infection to productive infection in tonsil CD4 T cells is modest, at less than 3% (Fig. S2A and B). In fact, most of the cells remain resistant to productive infection, likely reflecting the action of other restriction factors. In contrast to our initial hypothesis, Vpx degradation of SAMHD1 during HIV-2 infection does not lead to a rescue of HIV-associated cell death in the bystander population. Instead, killing in the HIV-2 cultures is enhanced, probably because more productively infected cells were present, promoting more effective spread of virus through cell-to-cell contacts. This enhancement of HIV-2 productive infection might be attributed to the Vpx-mediated release of SAMHD1 restriction at the reverse transcription stage but also could reflect Vpx depletion of the HUSH complex, which epigenetically represses the transcription of HIV proviruses (44). Bystander CD4 T cell death, which requires cell-to-cell transmission, was increased at early times in the HIV-2-infected cells likely due to the higher levels of productively

infected cells available for cell-to-cell transmission of virus in these cultures. At later time points, the number of productively infected cells became more comparable, and bystander killing occurred at similar levels in HIV-2-, HIV-2 ΔVpx-, and HIV-1-infected cultures. These findings did not support our hypothesis that the presence of Vpx would lead to diminished bystander cell death, but the different levels of productively infected cells in the infected cultures made interpretation of the results difficult. To remedy this problem, we utilized a 293T-HLAC overlay culture system, where the number of productively infected cells is quite similar. Again, we observed equivalent bystander CD4 T cell depletion in HIV-2- and HIV-2 ΔVpx-infected cultures. These findings clearly argued against our hypothesis that Vpx action would protect nonpermissive bystander CD4 T cells from pyroptotic programmed cell death.

We further found that forced encapsidation of exogenous Vpx protein into HIV-1 virions did not reduce levels of abortive infection and cell death occurring in bystander cells present in lymphoid tissue. Trinité et al. also showed that the introduction of Vpx protein in virus-like particles (VLPs) enhanced levels of viral reverse transcription in CD4 T cells isolated from blood (45). The reverse transcription did increase levels of productive infection in blood CD4 T cells, but Vpx did not prevent these cells from dying. Of note, a key difference in these results is that the blood-derived CD4 T cells studied by Trinité et al. died by noninflammatory apoptosis, while the CD4 T cells from lymphoid tissue died by inflammatory pyroptosis. Additionally, death of the blood CD4 T cells did not appear to be dependent on cell-to-cell transmission since single-round viruses were effective. In contrast, induction of pyroptosis in tonsil HLACs requires cell-to-cell virus transmission between productive infected cells and bystander cells. It is intriguing to consider the possibility that the precise mechanism of cell death elicited by HIV may differ in blood and lymphoid tissue. However, most of the pathogenic effects of HIV, including bystander CD4 T cell depletion, occur in lymphoid tissue, and progressive HIV disease is associated with chronic inflammation.

In summary, we show that CD4 T cell depletion in HIV-2-infected HLACs chiefly involves abortive infection, followed by pyroptosis, based on its inhibition by the entry inhibitor AMD3100 but not by the integrase inhibitor raltegravir, and by selective caspase-1 inhibitors. Together, our findings indicate that HIV-2 Vpx-mediated degradation of SAMHD1 does not influence the level of pyroptosis occurring during abortive infection and does not account for the reduced pathogenicity of HIV-2 in infected people. Indeed, both HIV-1 and HIV-2 deplete CD4 T cells through pyroptosis despite Vpx-induced SAMHD1 degradation. The host factors responsible for the different clinical courses of HIV-1 and HIV-2 remain unclear.

However, the fact that bystander CD4 T cells remain resistant to productive infection following HIV-2 infection raises the possibility that another restriction factor distinct from SAMHD1 remains active. Restriction at the level of nuclear import or prior to integration within the nucleus could lead to sensing of HIV DNA by IFI16, triggering pyroptotic cell death. Additionally, while HIV-2 induces comparable levels of abortive infection and cell death in CD4 T cells, Vpx-mediated degradation of SAMHD1 in macrophages or other myeloid cells perhaps plays an important role in the more benign clinical course of HIV-2 disease.

MATERIALS AND METHODS

Cells and medium supplements. Human tonsil specimens were obtained during routine tonsillectomies mainly for sleep disorders and supplied by the National Disease Research Interchange or the Cooperative Human Tissue Network. These tissues were processed as previously described (31). Briefly, tonsil tissue was dissected and pressed through a 40-μm mesh to create a single-cell suspension. Live HLACs were isolated by Ficoll density gradient centrifugation. CD4 T cells were isolated by negative selection using CD4 T cell isolation kits (catalog no. 130096533) from Miltenyi. HLACs were cultured in tonsil culture media, as previously described (31). The 293T and THP-1 cells were obtained from the American Tissue Culture Collection. The TZM-bl cell line, a generous gift from John C. Kappes, Xiaoyun Wu, and Tranzyme, Inc. (46), was obtained from the NIH AIDS Reagent Program, Division of AIDS, NIAID, NIH. 293T and TZM-bl cells were maintained in Dulbecco's modified Eagle's medium (DMEM). THP-1 cells were maintained in RPMI 1640 medium. All culture media were purchased from Corning and supplemented with 10% fetal bovine serum (FBS) from Corning and 1% penicillin-streptomycin-glutamine from Gemini.

Antibodies and reagents. Rabbit anti-SAMHD1 antibody (A303-691A) used for immunoblotting was purchased from Bethyl Laboratories. Mouse anti-SAMHD1 antibody (ab67820) used for flow cytometric staining was obtained from Abcam. Mouse anti-phospho (Thr592) anti-SAMHD1 antibody (8005) was purchased from ProSc. Mouse anti-β-actin antibody (A5316) was purchased from Sigma-Aldrich. Phycoerythrin (PE)-conjugated mouse anti-CD4 antibody (340670), antigen-presenting cell (APC)-conjugated mouse anti-CD8 antibody (340584), and APC-H7-conjugated mouse anti-CD2 antibody (562638) were purchased from BD Biosciences. Zombie Aqua fixable viability kits (catalog no. 423102) were purchased from BioLegend. AMD3100 octahydrochloride hydrate (A5602) was purchased from Sigma-Aldrich. Raltegravir (catalog no. sc-208296) was purchased from Santa Cruz Biotech. A selective caspase-1 inhibitor, Z-WEHD-FMK (FMK002), and a selective caspase-3 inhibitor, Z-DEVD-FMK (FMK004), were obtained from R&D Systems. Cell extraction buffer (catalog no. FNN0011) was purchased from Thermo Fisher Scientific. Protease inhibitor (catalog no. 04693132001) and phosphatase inhibitor (catalog no. 04906845001) were obtained from Roche.

Virus preparation. Proviral expression vector DNA corresponding to pNLENG1-IRES, pROD2-GFP, and pROD2-ΔVPX-GFP reporter viruses was transfected into 293T cells using the FuGENE HD transfection reagent from Promega. The medium was replaced after 16 h, and culture supernatants were collected every 24 h for 2 days. Virions were concentrated by ultracentrifugation. HIV-1 stocks were quantitated by measuring p24 gag levels by enzyme-linked immunosorbent assay (ELISA). The infectivity of each viral stock was measured by determining the 50% tissue culture infective dose ($TCID_{50}$) in TZM-bl cells (46, 47). The pNLENG1-IRES clone was derived from NL4-3, as previously described (48). HIV-2 Rod2-GFP and HIV-2 Rod2-ΔVPX-GFP clones, based on pRod9-ΔEnv-GFP and pRod9-ΔEnv-ΔVPX-GFP from M. Emerman, were generated by reintroduction of Rod9 Env.

HLAC spinoculation. HLACs were mixed with 50 ng p24 gag of HIV-1 (NLENG1-IRES). The $TCID_{50}$s of HIV-2 ROD2-GFP or HIV2 ROD2-ΔVPX-GFP viral preparations were determined using TZM-bl cells, allowing the delivery of equivalent infectious doses to use with HIV-1 (46). The infections for all three viruses were carried out using 1 million cells in a 100-μl total volume cultured in V-bottom wells of a 96-well plate. Cells were subjected to centrifugation (1,200 $\times$ *g*) for 2 h at 25°C and then cultured at 37°C as a pellet for up to 10 days until the experiment was terminated (30).

HLAC 293T overlay assay. To compare the killing of several single-round viruses from a comparable number of productively infected cells, we used a 293T cell overlay system, as previously described (33). In this system, transfected 293T cells serve as productively infected donor cells that can induce bystander killing of target HLAC cells through direct cell-to-cell transmission of virus. Briefly, a monolayer of 293T cells in 24-well plates were transfected with 50 ng HIV-1 (NLENG1-IRES), HIV-2 ROD2-GFP, or HIV2 ROD2-ΔVPX-GFP expression vector DNA. Four and a half million HLAC cells were pretreated with desired drugs and overlaid on 293T cells in the presence or absence of the desired antiviral drugs or caspase inhibitors. To restrict the infection to a single round, an integrase inhibitor (raltegravir) was added to HLACs 2 h before and during the overlay. The working concentrations were raltegravir, 15 μM; AMD3100, 0.2 to 2 mM; caspase-1 inhibitor Z-WEHD-FMK, 100 μM; and caspase-3 inhibitor Z-DEVD-FMK, 100 μM. HLACs were collected 1 to 3 days postcoculture (when more than 50% CD4 T cell killing was observed in the untreated or DMSO control) and assessed for percentage of CD4 T cell depletion. Replication-competent virus produced by each HIV-transfected 293T cultures were collected after 1 to 3 days and infectivity assessed in TZM-bl assays (data not shown). To incorporate Vpx protein into HIV-1 virions in *trans*, the HIV-1*.GFP proviral DNA and Vpx expression vectors (pcDNA3.1VpxSIVmac239-myc WT and Q76A) were graciously provided by Oliver T. Keppler (18, 22, 42). HIV-1*.GFP is modified from NL4-3 by insertion of a Vpx-binding motif, DPAVDLL, from macaque SIV (SIVmac) Gag into the Gag p6 region using overlapping PCR at the SpeI and SbfI sites of HIV-1 GFP. This mutation allows the packaging of exogenous Vpx protein into the virions (18). In the 293T overlay assay, we transfected 293T cells with HIV*.GFP and Vpx expression vector DNA at a 1:5 ratio (50 ng HIV-1*.GFP and 250 ng Vpx), followed by HLAC overlay.

FACS analysis and gating strategy. HLACs collected after spinoculation or HLAC 293T coculture assays were processed for fluorescence-activated cell sorting (FACS) staining using a live-dead cell discriminator dye (Zombie Aqua) and stained with fluorescently labeled antibodies specific for CD4, CD8, CD2, and SAMHD1. Data were collected on a LSR II flow cytometer from BD Biosciences and analyzed with the FlowJo software. Gating strategy, cell depletion calculation, and antibody validation are shown in Fig. S1.

Immunoblotting. THP-1, HLACs, isolated $CD4^+$ and $CD4^-$ HLACs, or HIV-1 or HIV-2-infected HLACs were collected and lysed in cell extraction buffer supplemented with phosphatase and protease inhibitors. Input protein was measured using a bicinchoninic acid (BCA) protein assay kit (catalog no. 23227) from Thermo Fisher Scientific. Samples were mixed with loading buffer (catalog no. LB0100) from Morganville Scientific and loaded onto a NuPAGE Novex 4 to 12% Bis-Tris protein gel (catalog no. NP0335BOX) from Life Technologies electrophoresed at 100 V. Proteins were wet transferred onto polyvinylidene difluoride (PVDF) membranes (catalog no. 162-0177) obtained from Bio-Rad. Immunoblotting with specific antibodies was performed, followed by corresponding secondary anti-rabbit IgG (catalog no. 32460) or anti-mouse IgG (catalog no. 32430) at a 1:5,000 dilution. The membrane was developed using a 1/4 dilution of SuperSignal (catalog no. 34095) from Thermo Scientific.

SUPPLEMENTAL MATERIAL

Supplemental material for this article may be found at https://doi.org/10.1128/JVI.00666-19.

SUPPLEMENTAL FILE 1, PDF file, 0.7 MB.

ACKNOWLEDGMENTS

We thank David N. Levy of NYU for the multiple-round NLENG1-IRES HIV reporter clones, M. Emerman for the Rod9-ΔEnv-GFP and Rod9-ΔEnv-ΔVPX-GFP HIV-2 reporter clones, and Oliver T. Keppler for HIV-1*.GFP proviral DNA and Vpx expression vectors (pcDNA3.1VpxSIVmac239-myc WT and Q76A). We thank John C. Kappes, Xiaoyun Wu, and Tranzyme, Inc., for TZM-bl cells donated to the NIH AIDS Reagent Program, Division of AIDS, NIAID, NIH. We are grateful for technical assistance from the Gladstone Flow Cytometry Core, including that of Marielle Cavrois and Nandhini Rahman. We thank Mauricio Montano for technical advice and stimulating discussions and Robin Givens and Sue Cammack for administrative assistance. Special thanks to Jason Neidleman for comments and revisions. We thank John C. W. Carroll and Giovanni Maki for graphic arts.

This work was made possible by funding from the Gladstone Institutes, the James B. Pendleton Charitable Trust, the UCSF-Gladstone Center for AIDS Research (NIH grant P30 AI027763), and NIH grants PO1AI124912, S10 RR028962, and R01 DA044605.

REFERENCES

1. McCune JM. 2001. The dynamics of CD4$^+$ T-cell depletion in HIV disease. Nature 410:974–979. https://doi.org/10.1038/35073648.
2. Masur H, Ognibene FP, Yarchoan R, Shelhamer JH, Baird BF, Travis W, Suffredini AF, Deyton L, Kovacs JA, Falloon J. 1989. CD4 counts as predictors of opportunistic pneumonias in human immunodeficiency virus (HIV) infection. Ann Intern Med 111:223–231. https://doi.org/10.7326/0003-4819-111-3-223.
3. Giorgi JV, Fahey JL, Smith DC, Hultin LE, Cheng HL, Mitsuyasu RT, Detels R. 1987. Early effects of HIV on CD4 lymphocytes in vivo. J Immunol 138:3725–3730.
4. Brenchley JM, Schacker TW, Ruff LE, Price DA, Taylor JH, Beilman GJ, Nguyen PL, Khoruts A, Larson M, Haase AT, Douek DC. 2004. CD4$^+$ T cell depletion during all stages of HIV disease occurs predominantly in the gastrointestinal tract. J Exp Med 200:749–759. https://doi.org/10.1084/jem.20040874.
5. Marlink R, Kanki P, Thior I, Travers K, Eisen G, Siby T, Traore I, Hsieh CC, Dia MC, Gueye EH. 1994. Reduced rate of disease development after HIV-2 infection as compared to HIV-1. Science 265:1587–1590. https://doi.org/10.1126/science.7915856.
6. Popper SJ, Sarr AD, Travers KU, Gueye-Ndiaye A, Mboup S, Essex ME, Kanki PJ. 1999. Lower human immunodeficiency virus (HIV) type 2 viral load reflects the difference in pathogenicity of HIV-1 and HIV-2. J Infect Dis 180:1116–1121. https://doi.org/10.1086/315010.
7. Berry N, Jaffar S, Schim van der Loeff M, Ariyoshi K, Harding E, N'Gom PT, Dias F, Wilkins A, Ricard D, Aaby P, Tedder R, Whittle H. 2002. Low level viremia and high CD4% predict normal survival in a cohort of HIV type-2-infected villagers. AIDS Res Hum Retroviruses 18:1167–1173. https://doi.org/10.1089/08892220260387904.
8. van der Loeff MF, Larke N, Kaye S, Berry N, Ariyoshi K, Alabi A, van Tienen C, Leligdowicz A, Sarge-Njie R, da Silva Z, Jaye A, Ricard D, Vincent T, Jones SR, Aaby P, Jaffar S, Whittle H. 2010. Undetectable plasma viral load predicts normal survival in HIV-2-infected people in a West African village. Retrovirology 7:46. https://doi.org/10.1186/1742-4690-7-46.
9. Andersson S, Norrgren H, da Silva Z, Biague A, Bamba S, Kwok S, Christopherson C, Biberfeld G, Albert J. 2000. Plasma viral load in HIV-1 and HIV-2 singly and dually infected individuals in Guinea-Bissau, West Africa: significantly lower plasma virus set point in HIV-2 infection than in HIV-1 infection. Arch Intern Med 160:3286–3293. https://doi.org/10.1001/archinte.160.21.3286.
10. MacNeil A, Sarr AD, Sankale JL, Meloni ST, Mboup S, Kanki P. 2007. Direct evidence of lower viral replication rates in vivo in human immunodeficiency virus type 2 (HIV-2) infection than in HIV-1 infection. J Virol 81:5325–5330. https://doi.org/10.1128/JVI.02625-06.
11. Jaffar S, Wilkins A, Ngom PT, Sabally S, Corrah T, Bangali JE, Rolfe M, Whittle HC. 1997. Rate of decline of percentage CD4$^+$ cells is faster in HIV-1 than in HIV-2 infection. J Acquir Immune Defic Syndr Hum Retrovirol 16:327–332. https://doi.org/10.1097/00042560-199712150-00003.
12. Camacho RJ. 2012. Special aspects of the treatment of HIV-2-infected patients. Intervirology 55:179–183. https://doi.org/10.1159/000332025.
13. de Silva TI, Cotten M, Rowland-Jones SL. 2008. HIV-2: the forgotten AIDS virus. Trends Microbiol 16:588–595. https://doi.org/10.1016/j.tim.2008.09.003.
14. Schim van der Loeff MF, Jaffar S, Aveika AA, Sabally S, Corrah T, Harding E, Alabi A, Bayang A, Ariyoshi K, Whittle HC. 2002. Mortality of HIV-1, HIV-2 and HIV-1/HIV-2 dually infected patients in a clinic-based cohort in The Gambia. AIDS 16:1775–1783. https://doi.org/10.1097/00002030-200209060-00010.
15. Brites C, Sampalo J, Oliveira A. 2009. HIV/human T-cell lymphotropic virus coinfection revisited: impact on AIDS progression. AIDS Rev 11:8–16.
16. Esbjörnsson J, Mansson F, Kvist A, Isberg PE, Nowroozalizadeh S, Biague AJ, da Silva ZJ, Jansson M, Fenyo EM, Norrgren H, Medstrand P. 2012. Inhibition of HIV-1 disease progression by contemporaneous HIV-2 infection. N Engl J Med 367:224–232. https://doi.org/10.1056/NEJMoa1113244.
17. Lahouassa H, Daddacha W, Hofmann H, Ayinde D, Logue EC, Dragin L, Bloch N, Maudet C, Bertrand M, Gramberg T, Pancino G, Priet S, Canard B, Laguette N, Benkirane M, Transy C, Landau NR, Kim B, Margottin-Goguet F. 2012. SAMHD1 restricts the replication of human immunodeficiency virus type 1 by depleting the intracellular pool of deoxynucleoside triphosphates. Nat Immunol 13:223–228. https://doi.org/10.1038/ni.2236.
18. Baldauf HM, Pan X, Erikson E, Schmidt S, Daddacha W, Burggraf M, Schenkova K, Ambiel I, Wabnitz G, Gramberg T, Panitz S, Flory E, Landau NR, Sertel S, Rutsch F, Lasitschka F, Kim B, Konig R, Fackler OT, Keppler OT. 2012. SAMHD1 restricts HIV-1 infection in resting CD4$^+$ T cells. Nat Med 18:1682–1687. https://doi.org/10.1038/nm.2964.
19. Goldstone DC, Ennis-Adeniran V, Hedden JJ, Groom HC, Rice GI, Christodoulou E, Walker PA, Kelly G, Haire LF, Yap MW, de Carvalho LP, Stoye JP, Crow YJ, Taylor IA, Webb M. 2011. HIV-1 restriction factor SAMHD1 is a deoxynucleoside triphosphate triphosphohydrolase. Nature 480:379–382. https://doi.org/10.1038/nature10623.
20. Yu XF, Yu QC, Essex M, Lee TH. 1991. The vpx gene of simian immunodeficiency virus facilitates efficient viral replication in fresh lymphocytes and macrophage. J Virol 65:5088–5091.
21. Yu XF, Ito S, Essex M, Lee TH. 1988. A naturally immunogenic virion-associated protein specific for HIV-2 and SIV. Nature 335:262–265. https://doi.org/10.1038/335262a0.
22. Baldauf HM, Stegmann L, Schwarz SM, Ambiel I, Trotard M, Martin M, Burggraf M, Lenzi GM, Lejk H, Pan X, Fregoso OI, Lim ES, Abraham L, Nguyen LA, Rutsch F, Konig R, Kim B, Emerman M, Fackler OT, Keppler OT. 2017. Vpx overcomes a SAMHD1-independent block to HIV reverse transcription that is specific to resting CD4 T cells. Proc Natl Acad Sci U S A 114:2729–2734. https://doi.org/10.1073/pnas.1613635114.
23. Wu L. 2012. SAMHD1: a new contributor to HIV-1 restriction in resting CD4$^+$ T-cells. Retrovirology 9:88. https://doi.org/10.1186/1742-4690-9-88.
24. St Gelais C, Kim SH, Maksimova VV, Buzovetsky O, Knecht KM, Shepard C, Kim B, Xiong Y, Wu L. 2018. A cyclin-binding motif in human SAMHD1 is required for its HIV-1 restriction, dNTPase activity, tetramer formation,

and efficient phosphorylation. J Virol 92:e01787-17. https://doi.org/10.1128/JVI.01787-17.
25. Valle-Casuso JC, Allouch A, David A, Lenzi GM, Studdard L, Barré-Sinoussi F, Müller-Trutwin M, Kim B, Pancino G, Sáez-Cirión A. 2017. p21 restricts HIV-1 in monocyte-derived dendritic cells through the reduction of deoxynucleoside triphosphate biosynthesis and regulation of SAMHD1 antiviral activity. J Virol 91:e01324-17. https://doi.org/10.1128/JVI.01324-17.
26. Dragin L, Nguyen LA, Lahouassa H, Sourisce A, Kim B, Ramirez BC, Margottin-Goguet F. 2013. Interferon block to HIV-1 transduction in macrophages despite SAMHD1 degradation and high deoxynucleoside triphosphates supply. Retrovirology 10:30. https://doi.org/10.1186/1742-4690-10-30.
27. Li J, Xu F, Hu S, Zhou J, Mei S, Zhao X, Cen S, Jin Q, Liang C, Guo F. 2015. Characterization of the interactions between SIVrcm Vpx and red-capped mangabey SAMHD1. Biochem J 468:303–313. https://doi.org/10.1042/BJ20141331.
28. Shingai M, Welbourn S, Brenchley JM, Acharya P, Miyagi E, Plishka RJ, Buckler-White A, Kwong PD, Nishimura Y, Strebel K, Martin MA. 2015. The expression of functional Vpx during pathogenic SIVmac infections of rhesus macaques suppresses SAMHD1 in CD4$^+$ memory T cells. PLoS Pathog 11:e1004928. https://doi.org/10.1371/journal.ppat.1004928.
29. Chougui G, Munir-Matloob S, Matkovic R, Martin MM, Morel M, Lahouassa H, Leduc M, Ramirez BC, Etienne L, Margottin-Goguet F. 2018. HIV-2/SIV viral protein X counteracts HUSH repressor complex. Nat Microbiol 3:891–897. https://doi.org/10.1038/s41564-018-0179-6.
30. Doitsh G, Cavrois M, Lassen KG, Zepeda O, Yang Z, Santiago ML, Hebbeler AM, Greene WC. 2010. Abortive HIV infection mediates CD4 T cell depletion and inflammation in human lymphoid tissue. Cell 143:789–801. https://doi.org/10.1016/j.cell.2010.11.001.
31. Doitsh G, Galloway NL, Geng X, Yang Z, Monroe KM, Zepeda O, Hunt PW, Hatano H, Sowinski S, Munoz-Arias I, Greene WC. 2014. Cell death by pyroptosis drives CD4 T-cell depletion in HIV-1 infection. Nature 505:509–514. https://doi.org/10.1038/nature12940.
32. Doitsh G, Greene WC. 2016. Dissecting how CD4 T cells are lost during HIV infection. Cell Host Microbe 19:280–291. https://doi.org/10.1016/j.chom.2016.02.012.
33. Galloway NL, Doitsh G, Monroe KM, Yang Z, Munoz-Arias I, Levy DN, Greene WC. 2015. Cell-to-cell transmission of HIV-1 is required to trigger pyroptotic death of lymphoid-tissue-derived CD4 T cells. Cell Rep 12:1555–1563. https://doi.org/10.1016/j.celrep.2015.08.011.
34. Monroe KM, Yang Z, Johnson JR, Geng X, Doitsh G, Krogan NJ, Greene WC. 2014. IFI16 DNA sensor is required for death of lymphoid CD4 T cells abortively infected with HIV. Science 343:428–432. https://doi.org/10.1126/science.1243640.
35. Descours B, Cribier A, Chable-Bessia C, Ayinde D, Rice G, Crow Y, Yatim A, Schwartz O, Laguette N, Benkirane M. 2012. SAMHD1 restricts HIV-1 reverse transcription in quiescent CD4$^+$ T-cells. Retrovirology 9:87. https://doi.org/10.1186/1742-4690-9-87.
36. Muñoz-Arias I, Doitsh G, Yang Z, Sowinski S, Ruelas D, Greene WC. 2015. Blood-derived CD4 T cells naturally resist pyroptosis during abortive HIV-1 infection. Cell Host Microbe 18:463–470. https://doi.org/10.1016/j.chom.2015.09.010.
37. Cribier A, Descours B, Valadao AL, Laguette N, Benkirane M. 2013. Phosphorylation of SAMHD1 by cyclin A2/CDK1 regulates its restriction activity toward HIV-1. Cell Rep 3:1036–1043. https://doi.org/10.1016/j.celrep.2013.03.017.
38. Khalid M, Yu H, Sauter D, Usmani SM, Schmokel J, Feldman J, Gruters RA, van der Ende ME, Geyer M, Rowland-Jones S, Osterhaus AD, Kirchhoff F. 2012. Efficient Nef-mediated downmodulation of TCR-CD3 and CD28 is associated with high CD4$^+$ T cell counts in viremic HIV-2 infection. J Virol 86:4906–4920. https://doi.org/10.1128/JVI.06856-11.
39. Chen P, Hubner W, Spinelli MA, Chen BK. 2007. Predominant mode of human immunodeficiency virus transfer between T cells is mediated by sustained Env-dependent neutralization-resistant virological synapses. J Virol 81:12582–12595. https://doi.org/10.1128/JVI.00381-07.
40. Carr JM, Hocking H, Li P, Burrell CJ. 1999. Rapid and efficient cell-to-cell transmission of human immunodeficiency virus infection from monocyte-derived macrophages to peripheral blood lymphocytes. Virology 265:319–329. https://doi.org/10.1006/viro.1999.0047.
41. Nyamweya S, Hegedus A, Jaye A, Rowland-Jones S, Flanagan KL, Macallan DC. 2013. Comparing HIV-1 and HIV-2 infection: lessons for viral immunopathogenesis. Rev Med Virol 23:221–240. https://doi.org/10.1002/rmv.1739.
42. Gramberg T, Sunseri N, Landau NR. 2010. Evidence for an activation domain at the amino terminus of simian immunodeficiency virus Vpx. J Virol 84:1387–1396. https://doi.org/10.1128/JVI.01437-09.
43. Unterholzner L, Keating SE, Baran M, Horan KA, Jensen SB, Sharma S, Sirois CM, Jin T, Latz E, Xiao TS, Fitzgerald KA, Paludan SR, Bowie AG. 2010. IFI16 is an innate immune sensor for intracellular DNA. Nat Immunol 11:997–1004. https://doi.org/10.1038/ni.1932.
44. Yurkovetskiy L, Guney MH, Kim K, Goh SL, McCauley S, Dauphin A, Diehl WE, Luban J. 2018. Primate immunodeficiency virus proteins Vpx and Vpr counteract transcriptional repression of proviruses by the HUSH complex. Nat Microbiol 3:1354–1361. https://doi.org/10.1038/s41564-018-0256-x.
45. Trinité B, Chan CN, Lee CS, Levy DN. 2016. HIV-1 Vpr- and reverse transcription-induced apoptosis in resting peripheral blood CD4 T cells and protection by common gamma-chain cytokines. J Virol 90:904–916. https://doi.org/10.1128/JVI.01770-15.
46. Platt EJ, Bilska M, Kozak SL, Kabat D, Montefiori DC. 2009. Evidence that ecotropic murine leukemia virus contamination in TZM-bl cells does not affect the outcome of neutralizing antibody assays with human immunodeficiency virus type 1. J Virol 83:8289–8292. https://doi.org/10.1128/JVI.00709-09.
47. Sarzotti-Kelsoe M, Bailer RT, Turk E, Lin CL, Bilska M, Greene KM, Gao H, Todd CA, Ozaki DA, Seaman MS, Mascola JR, Montefiori DC. 2014. Optimization and validation of the TZM-bl assay for standardized assessments of neutralizing antibodies against HIV-1. J Immunol Methods 409:131–146. https://doi.org/10.1016/j.jim.2013.11.022.
48. Trinité B, Chan CN, Lee CS, Mahajan S, Luo Y, Muesing MA, Folkvord JM, Pham M, Connick E, Levy DN. 2014. Suppression of Foxo1 activity and down-modulation of CD62L (L-selectin) in HIV-1 infected resting CD4 T cells. PLoS One 9:e110719. https://doi.org/10.1371/journal.pone.0110719.